24th COBEM - 2017

24th ABCM International Congress of Mechanical Engineering
December 3-8, 2017, Curitiba, PR, Brazil

COBEM-2017-1176
DESIGN OF AN EMBEDDED SYSTEM FOR WATER TEMPERATURE CONTROL IN A SOLAR ASSISTED HEAT PUMP

Tiago de Freitas Paulino
Graduate Program in Mechanical Engineering, Federal University of Minas Gerais, Av. Antônio Carlos , 6627, Pampulha, 31270-901, Belo Horizonte (MG), Brazil
Department of Materials Engineering, Federal Center of Technological Education of Minas Gerais, Av. Amazonas, 5253, Nova Suiça, 30421-169, Belo Horizonte (MG), Brazil
tfpaulinoeng@gmail.com

Euler Assunção Costa Fonseca
Department of Mechanical Engineering, Federal University of Minas Gerais, Av. Antônio Carlos , 6627, Pampulha, 31270-901, Belo Horizonte (MG), Brazil
fcaeuler@gmail.com

Antônio Augusto Torres Maia
Luiz Machado
Ricardo Nicolau Nassar Koury
Graduate Program in Mechanical Engineering, Federal University of Minas Gerais, Av. Antônio Carlos , 6627, Pampulha, 31270-901, Belo Horizonte (MG), Brazil
aamaia@demec.ufmg.br, luizm@demec.ufmg.br, koury@demec.ufmg.br

Abstract. *The heat pump is considered as one of the alternatives to achieve greater efficiency in heating water for bath. The control of heating water is necessary in a direct expansion solar assisted heat pump (DX-SAHP) for proper operation. One of the alternatives to make the control effective would be an embedded system. In this study, it is presented a low cost embedded system which is developed to set the hot water temperature in 60°C in a DX-SAHP. The hardware of the embedded system has a microcontroller, an optocoupler for separating power and control circuits, a Mosfet for high frequency switching and a Schottky diode for attenuating the reverse current. The software has as its main functions getting temperature throughout an interruption generated by timer, the calculation of the error by comparing the current temperature with the set-point, the calculation of the PID, the generation of PWM signal and finally, the data is displayed on the LCD and sent by USB port. The system performance was verified with a solar radiation variation between 154 W/m² and 1154 W/m². During this test the maximum absolute error (MAE) and the root mean square error (RMSE) were 1.25 and 0.028, respectively. The volumetric flow rate varied between 0.26 L/min and 0.55 L/min during the solar radiation variation to keep the hot water temperature in the correct value.*

Keywords: *control water temperature, embedded system, heat pump, solar assisted*

1. INTRODUCTION

The hot water in residences generally has a high cost to be obtained due to the significant consume of energy. In general, water heating is produced by electricity or by gas. Vasconcellos and Limberger (2012) report that the electric shower is estimated to contribute 24% of residential electricity consumption in Brazil. In the last years, the market of water heating is more and more demanding for more rational use of energy and for reducing the emission of greenhouse gas.

An alternative to have a more efficient system for water heating is the use of heat pumps. For producing hot water the heat pump can be used as a complementary energy source (Reis et al., 2014) or as a main equipment (Hepbasli and Kalinci, 2009; Islam, Sumathy and Khan, 2013).

The use of heat pump for heating water reduces significantly the electricity consumption because this equipment uses thermal energy available in the environment. When the heat pump is direct expansion solar assisted it is possible to have the system operating at an even higher COP. Kong et al. (2011) and Sun et al. (2014) report the increase of the COP in the solar assisted heat pump.

For proper use of the carbon dioxide (CO_2) heat pump it is required two control systems. The first system acts to keep the water temperature in a suitable set point of 45°C for a direct consume as discussed by Shao et al. (2004) and 60°C for storage (Bensoussan et al., 2014). It is important to keep the system working in the correct set point because when the water temperature is lower, the outlet gas cooler temperature is lower and the COP is better (Yang et al., 2015). The second system acts to keep the high pressure at an adequate value through adjusts in the expansion device. In this study, the discussion is focused in the control of hot water temperature.

Choi (2013) presented a study about the control of hot water temperature in a water-water heat pump. Among the alternatives analyzed by the author, the modification of water mass flow rate is indicated as the solution that produces the highest COP, although it is not the option for the best refrigeration capacity. Minetto (2011) and Hu et al. (2015) also study the control of hot water temperature in the heat pump by changing the water mass flow rate.

The control of hot water temperature can be developed through programmable logic controller or by an embedded system. Considering that this type of heat pump is designed to be used in residences, the cost is an important factor. Therefore, the embedded system was chosen. In this study it is presented a low cost embedded system which is developed to control the hot water temperature in a DX-SAHP. The value estimated for commercial manufacture of the embedded system is less than 70 U$.

2. EXPERIMENTAL DEVICE

In Fig. 1 it is presented the CO_2 DX-SAHP used in this study. The main components are a needle valve (expansion device) (1), an evaporator/collector (2), a reciprocating compressor (3) and a gas cooler (4). The compressor was manufactured by SANDEN. The gas cooler consists of two concentric tubes where CO_2 and water flow in countercurrent. The needle valve model SS-31RS4 was manufactured by SWAGELOK. The evaporator / collector receives energy from natural and forced convection from the condensation of water vapor in the external atmospheric air and from solar radiation. The evaporator / collector was designed for a power of 700 W/m² and it has an area equal to 1.57 m².

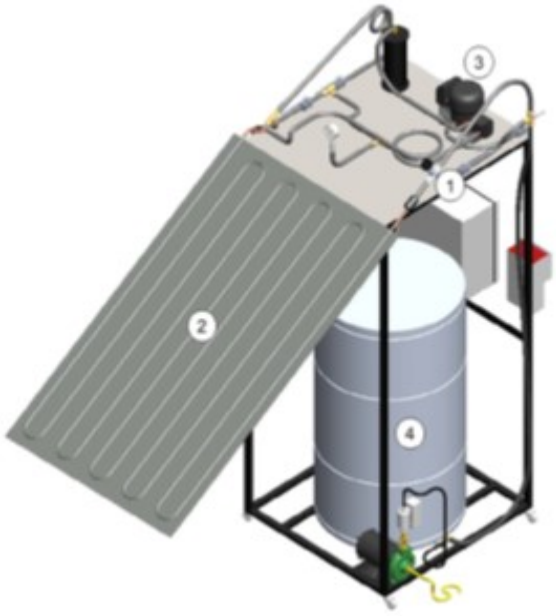

Figure 1. CO_2 DX-SAHP for water heating.

The water pump model 100-000-21 was manufactured by SHURflo. This pump provides a volumetric flow rate of 1 L/min at 0.7 bar and 12 Vdc and 1 A.

3. CONTROLLER DEVELOPMENT

The energy (Q_{CO2}) in the evaporator / collector changes during the day. The Eq. (1) shows the effect of this energy variation in the refrigerant. During this process, the difference between enthalpy (Δh) at the outlet (h_o) and at the inlet (h_i) of the evaporator is almost the same, but there is change in the mass flow rate (m_{CO2}) of CO_2. As a result, in the gas cooler the CO_2 will be able to deliver more energy to water. The Eq. (2) shows the heat transfer to water (Q_w), the inlet water temperature (T_{iw}) and specific heat of water at constant pressure (c_p) are constant, then, the water mass flow rate (m_w) needs to change for keeping the outlet water temperature (T_{ow}) at the appropriate value.

$$\dot{Q}_{CO2} = \dot{m}_{CO2}\Delta h = \dot{m}_{CO2}\left(h_o - h_i\right) \tag{1}$$

$$\dot{Q}_w = \dot{m}_w c_p \Delta T = \dot{m}_w c_p \left(T_{ow} - T_{iw}\right) \tag{2}$$

3.1 Control algorithm

According to Campos and Teixeira (2010) the controller proportional-integral-derivative (PID) is the most used in the industry for closed-loop system. The authors describe the advantages of PID control as good performance, versatile structure, low number of parameters to set or tune, and it is easy to associate parameters of setting and tuning. The Eq. (3) shows the implementation of classic parallel PID.

$$u(t) = K_p\left(e(t) + \frac{1}{T_I}\int_0^t e(t)dt + T_D\frac{de(t)}{dt}\right) \tag{3}$$

However, only discrete signal can be implemented in an embedded system. So, approximations were used for integral and derivative terms. The derivative term is approximated for Euler method as shows Eq. (4). The integral term is approximate by Tustin technique as shows Eq. (5). In this technique the integral, or area, between two points is approximate by a rectangle. The base of rectangle is the time and the height is the average temperature between the current time and the previous instant of time. The Eq. (5) also considers the integral in the previous instant of time. Therefore, the Eq. (3) is rewritten in the Eq. (6) and the Eq. (6) can be implemented in an embedded system.

$$\frac{de(t)}{dt} \cong \frac{e(kT) - e(kT - T)}{T} \tag{4}$$

$$\int_0^t e(t)dt \cong u(kT) = u(kT - T) + \frac{e(kT) + e(kT - T)}{2}T \tag{5}$$

$$u(t) \cong K_p e(t) + u(kT - T) + K_i\frac{e(kT) + e(kT - T)}{2}T + K_d\frac{e(kT) + e(kT - T)}{T} \tag{6}$$

In the Eq. (3), Eq. (4), Eq. (5) and Eq. (6) u is the controller output, t is the time, K_p is the proportional gain, K_i is the integral gain, K_d is the derivative gain, e is the error signal, T_I is the integration time, T_D is the derivative time, $e(t)$ is the error during the time, $e(kT)$ is the current error, $e(kT-T)$ is the error in the previous instant of time, $u(kT)$ is the controller output in the current time and $u(kT)$ is controller output in the previous instant of time.

Two methods were used to evaluate errors: maximum absolute error (MAE), as shows Eq. (7) and root mean square error (RMSE) calculated by Eq. (8). Where $T_{ow,i}$ is the current water temperature, $T_{ow,set}$ is the water temperature correct value and n is the number of points.

$$MAE = \max_i \left|T_{ow,i} - T_{ow,set}\right| \tag{7}$$

$$RMSE = \sqrt{\frac{\sum_{i=1}^{n}\left(T_{ow,i} - T_{ow,set}\right)^2}{n}} \tag{8}$$

3.2 Software description

The software developed to control the water temperature presents the following steps: first the initial configurations were done and after that the temperature is obtained throughout an interruption generated by timer. Having the current water temperature, this value is compared with the appropriate value and the error is sent to the function of PID controller. The output of the PID function is the input data to generate the pulse width modulation (PWM) signal.

Finally, the data is displayed on the LCD and sent by USB port for a computer. The constants used in the controller were 4.37, 0.18 and 6.51 for K_p, K_i and K_d respectively. Figure 2 shows the software flowchart.

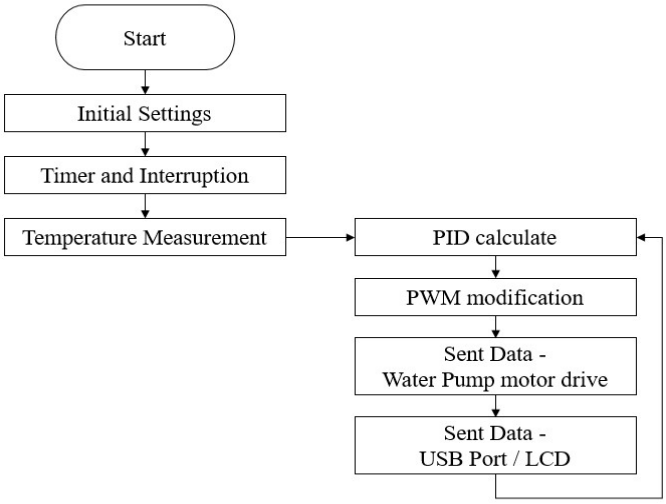

Figure 2. Software for hot water temperature control.

3.3 Hardware description

Figure 3 shows the hardware developed to control the hot water temperature. In order to separate power and control circuits, an optocoupler was used. Further, for switching in high frequency of the water pump DC motor a PWM signal is used. Because the switching occurs in high frequency, it is included a Schottky diode for attenuating the reverse current and improving the quality of PWM signal. In addition, a three ampere fuses for current limitation was included because of the recommendation of the water pump manufacturer. Finally, the sensor used for temperature measurement is the DS18b20.

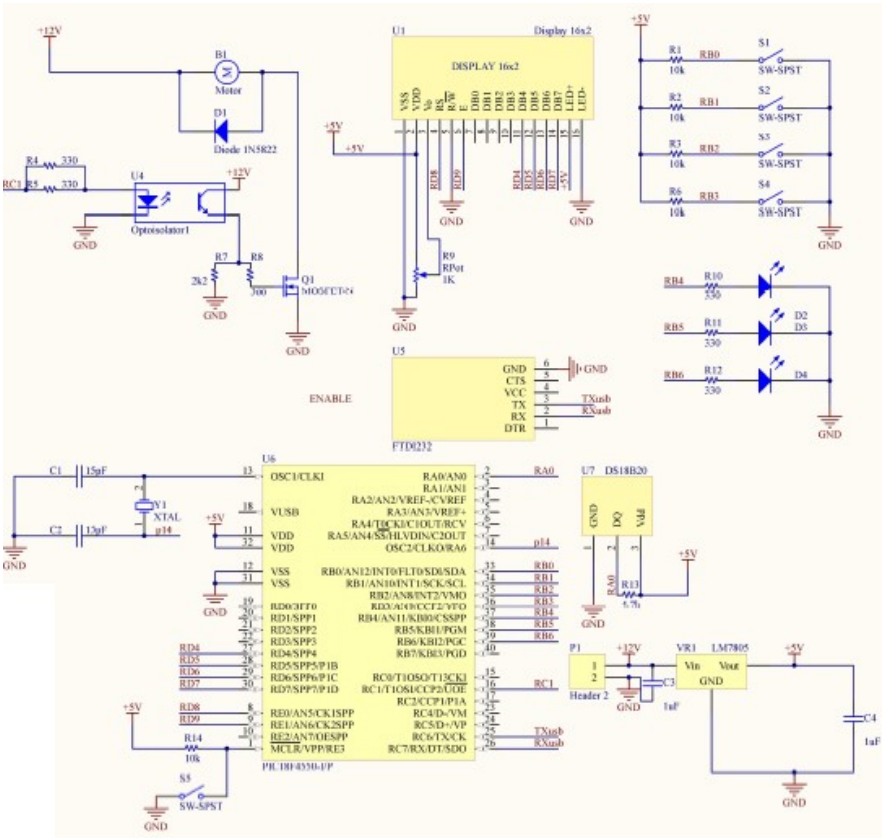

Figure 3. Hardware for hot water temperature control.

4. RESULTS AND DISCUSSION

4.1 Pulse width modulation signal

Figure 4 shows the curve for a PWM signal when the duty cycle is equal to 900. The duty cycle represents the part of the one period in which the signal is in high level. In this case, as the maximum duty cycle is 1023. If the duty cycle is equal to 900, the voltage DC sent to the system is ((900/1023)x12.8V), 11,2V as shows Fig. 4. Analyzing Fig. 4 it is also possible to notice a reasonable wave rectified because of the use of Schottky diode.

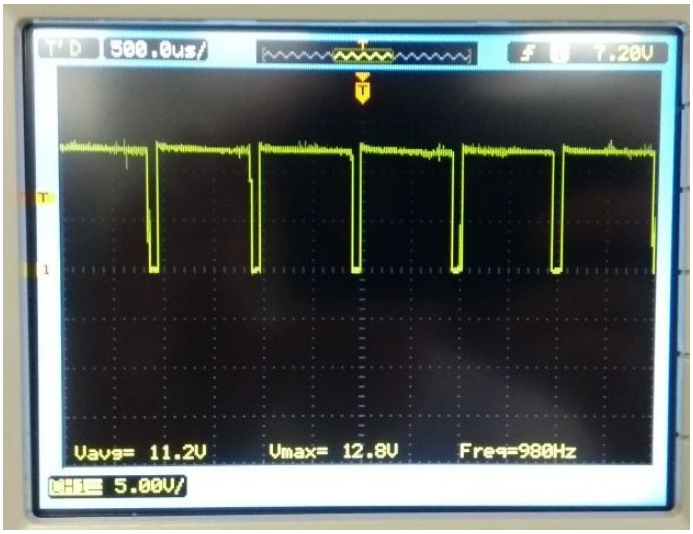

Figure 4. Oscilloscope signal.

4.2 Voltage and volumetric flow rate curve

An experimental work was performed to obtain the curves of the voltage and the volumetric flow rate as a function of the duty cycle. Figure 5 shows the results when a different duty cycle was sent to the drive motor. During the experiment the oscilloscope registered the current voltage and the volumetric flow rate was measured. The results presented in the Fig. 5 were used to generate the voltage and the volumetric flow rate curves from the duty cycle as represent Eq. (9) and Eq. (10) respectively.

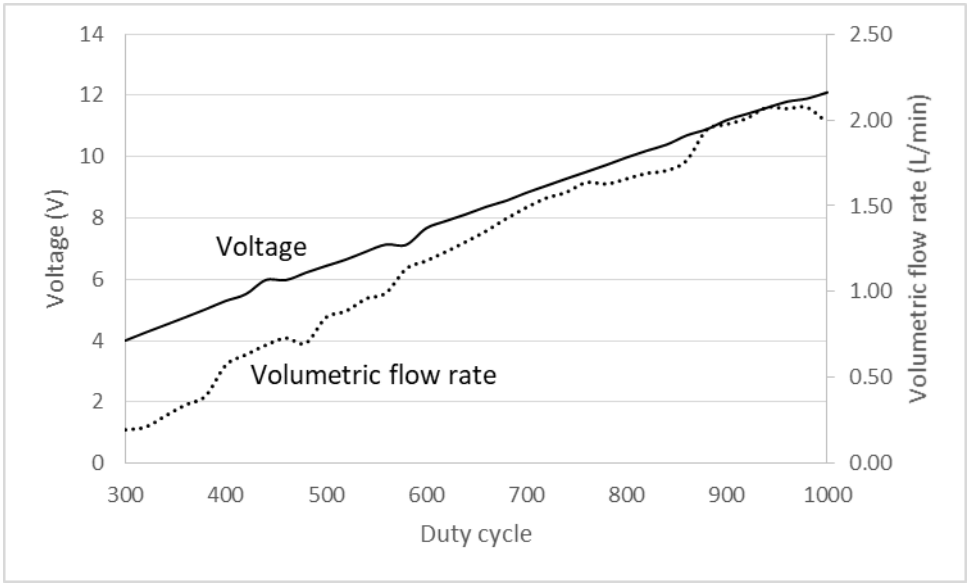

Figure 5. Voltage *versus* Duty cycle and Volumetric flow rate *versus* Duty cycle.

$$Voltage(V) = 0.0117 \times DutyCycle + 0.6046 \quad (9)$$

$$\dot{V}(L/\min) = 0.0028 \times DutyCycle - 0.5765 \tag{10}$$

4.3 Water temperature control

Figure 6 shows the water temperature control in the DX-SAHP during around 42 minutes. It is possible to notice that controller try to fix the water temperature in the correct value, 60°C. Additionally, in this experiment, after the hot water temperature achieve the correct value, the MAE and the RMSE were 1.25 and 0.028, respectively.

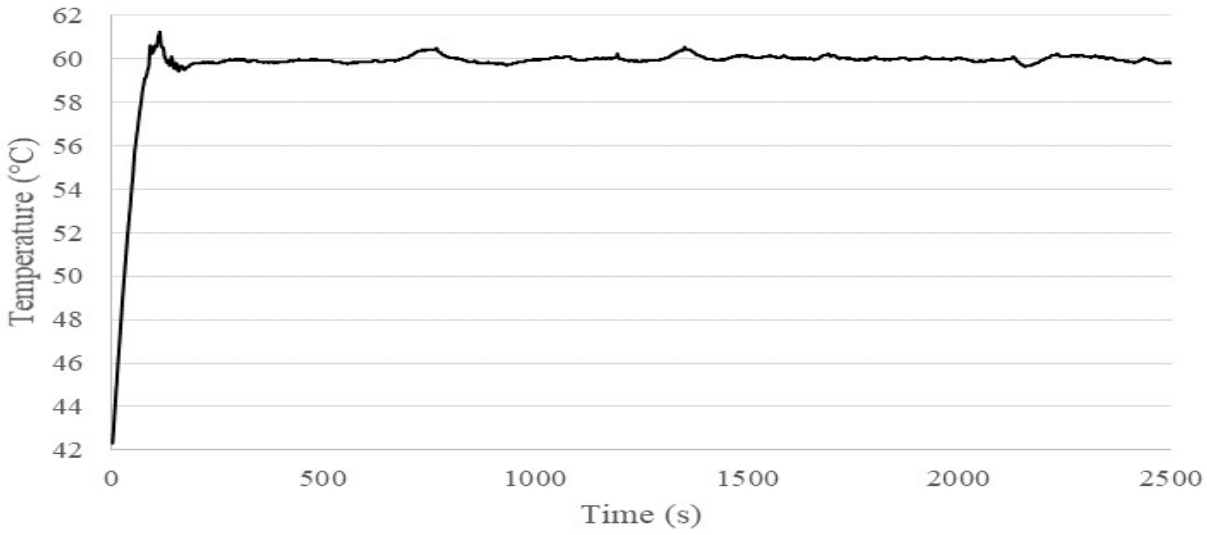

Figure 6. Hot water temperature control.

Figure 7 shows the temperature and volumetric flow rate during the experiment. The water mass flow rate (product of the volumetric flow rate and density) varies to keep the outlet water temperature in the correct value. During this time, there was a considerable variation in the solar radiation (154 W/m² - 1154 W/m²), due to the presence of clouds during the tests. Moreover, during the test the ambient temperature was around 25°C. This experiment was important to verify the adequacy of the controller in an environment condition that change all the time.

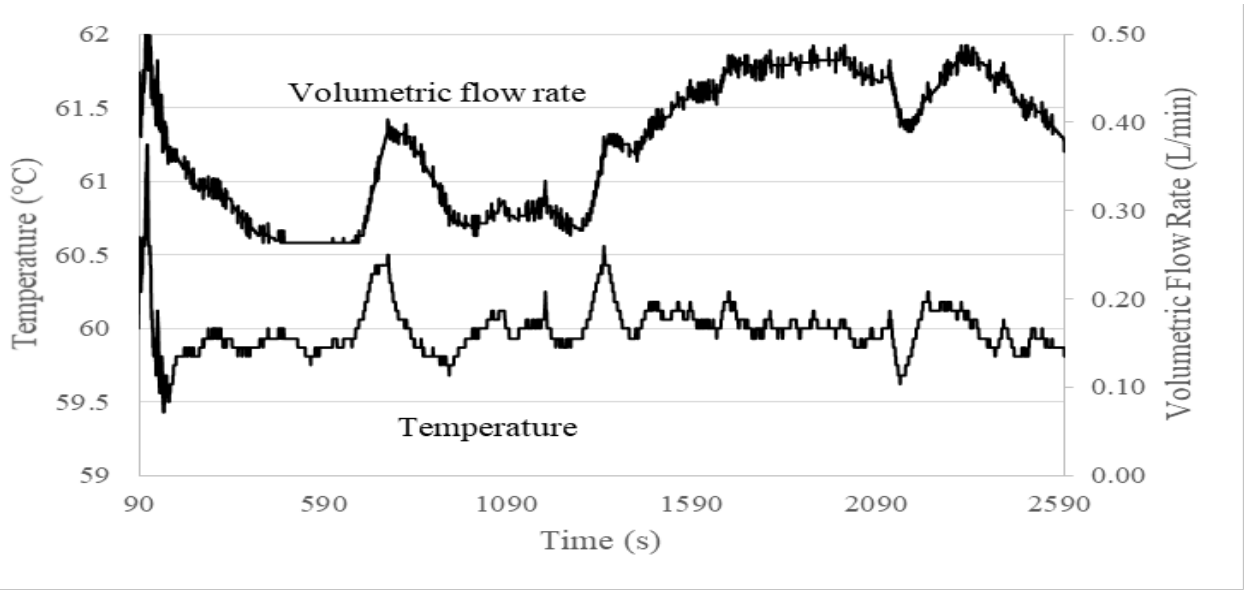

Figure 7. Hot water temperature control and Volumetric flow rate.

When the solar radiation is high, the volumetric flow rate is high. On the other hand, when the solar radiation is low the volumetric flow rate is low. As discussed before, when the amount of solar radiation that achieves the evaporator

increase, the CO_2 mass flow rate also increases. At this time, the mass flow rate of water should be augmented to preserve the water temperature at the desired set point. In the Fig. 5 can be observed the minimum (0.26 L/min) and the maximum (0.55 L/min) water volumetric flow rate realized during the tests.

5. CONCLUSIONS

This paper presents the low cost embedded system to set the hot water temperature in 60°C in a DX-SAHP. The software and hardware developed is presented. The performance of the system was verified for around 42 minutes in a day with considerable variation in the solar radiation (154 W/m² - 1154 W/m²). During this test, the MAE and the RMSE were 1.25 and 0.028, respectively. The volumetric flow rate varied between 0.26 L/min and 0.55 L/min during the solar radiation variation to keep the hot water in the correct value. The system worked as expected keeping the hot water in the correct value even with a widely variation in the solar radiation.

6. ACKNOWLEDGEMENTS

This work was supported by Fundação de Amparo à Pesquisa do Estado de Minas Gerais (FAPEMIG).

7. REFERENCES

Bensoussan, M.Á., 2014. *Legionella na Visão de Especialistas*. São Paulo: SETRI Consultoria em Sustentabilidade Ltda, 354 p.

Campos, M.C.M.M., Teixeira, H.C.G., 2010. *Controles Típicos de Equipamentos e Processos Industriais*. Blucler, 2nd edition, São Paulo.

Choi, J.M., 2013. *"Study on the LWT control schemes of a heat pump for hot water supply"*. Renewable Energy, Vol. 54, p. 20-25.

Hepbasli, A., Kalinci, Y., 2009. *"A review of heat pump water heating systems"*. Renewable and Sustainable Energy Reviews. Vol.13, p.1211–1229.

Hu, B., Li, Y., Cao, F., Xing, Z., 2015. "*Extremum seeking control of COP optimization for air-source transcritical CO_2 heat pump water heater system"*. Applied Energy, Vol. 147, p. 361–372.

Islam, M.R., Sumathy, K., Khan, S.U., 2013. *"Solar water heating systems and their market trends"*. Renewable and Sustainable Energy Reviews. Vol. 17, p. 1–25.

Kong, X.Q., Zhang, D., Li, Y., Yang, Q.M., 2011. *"Thermal performance analysis of a direct-expansion solar-assisted heat pump water heater"*. Energy, Vol. 36, p. 6830-6838.

Minetto, S., 2011. *"Theoretical and experimental analysis of a CO_2 heat pump for domestic hot water"*. International Journal of Refrigeration, Vol. 34, p. 742-751.

Reis, R.V.M., Maia, A.A.T., Machado, L., Koury, R.N.N., 2014. *"Comparative study between a heat pump and an electrical resistance as energy support for a solar water heater"*. Advanced Materials Research, Vol. 1016, p. 748-752.

Shao, S., Shi, W., Li, X., Ma, J., 2004. "A new inverter heat pump operated all year round with domestic hot water". Energy Conversion and Management. Vol. 45, p. 2255–2268.

Sun, X., Wu, J., Dai, Y., Wang, R., 2014. *"Experimental study on roll-bond collector/evaporator with optimized channel used in direct expansion solar assisted heat pump water heating system"*. Applied Thermal Engineering, Vol. 66, p. 571-579.

Vasconcellos, L.E.M., Limberger, M.A.C., 2012. *Energia Solar para aquecimento de água no Brasil: Contribuições da Eletrobrás Procel e Parceiros*. Eletrobrás, 240 p., Rio de Janeiro.

Yang, L., Li, H., Cai, S., Shao, L., Zhang, C., 2015. *"Minimizing COP loss from optimal high pressure correlation for transcritical CO_2 cycle".* Applied Thermal Engineering, Vol. 89, p. 656-662.

8. RESPONSIBILITY NOTICE

The authors are the only responsible for the printed material included in this paper.